Journal of Nuclear Materials 386–388 (2009) 483–486

Contents lists available at ScienceDirect

Journal of Nuclear Materials

journal homepage: www.elsevier.com/locate/jnucmat

High temperature characterization of LPS-SiC based materials with oxide additives

S.P. Lee [a,*], M.H. Lee [a], J.K. Lee [a], A. Kohyama [b], J.H. Lee [c]

[a] Department of Mechanical Engineering, Dong-Eui University, Busan 614-714, Republic of Korea
[b] Institute of Advanced Energy, Kyoto University, Kyoto 611-0011, Japan
[c] School of Mechanical Engineering, Pusan National University, Busan 609-735, Republic of Korea

A B S T R A C T

This paper dealt with the microstructure and the flexural strength of monolithic SiC and SiC_f/SiC composite materials. Especially, the mechanical property of SiC based materials were investigated at the elevated temperatures of 1000 and 1200 °C in the argon atmosphere. The microstructural variation of SiC based materials by the thermal exposure at the bending test temperature was also analyzed. SiC based materials were fabricated by a liquid phase sintering process (LPS), using an additive materials of Al_2O_3 and Y_2O_3. A two-dimensional weave of Tyranno SA fibers were utilized as a reinforcing material for SiC_f/SiC composite. SiC based materials was sintered at the temperature of 1820 °C for the creation of secondary phases. LPS-SiC materials represented a good density of about 3.1 Mg/m^3 and an average flexural strength of about 750 MPa at the room temperature. The sintering density of LPS-SiC_f/SiC was also similar to that of LPS-SiC materials. However, the flexural strength of LPS-SiC based materials greatly decreased with the increase of test temperature.

1. Introduction

SiC materials have been considered as a promising candidate for high temperature components, because of its excellent high temperature strength and good irradiation resistance. With the rapid development of high crystalline SiC fibers, SiC fiber reinforced SiC matrix composites (SiC_f/SiC) have been extensively studied for a new approach in the fusion power plant systems such as first wall or divertor coolant channel [1–3]. Recently, both the creation of high-purity SiC matrix and its densification in the intra-fiber bundle region must be still emphasized in the R&D fields of high performance SiC_f/SiC composites, since it can provide a good oxidation resistance and a high thermal conductivity at the elevated temperature. SiC_f/SiC composites have been fabricated by various methods such as reaction sintering (RS), liquid phase sintering (LPS) and hybrid process by the combination of RS and polymer impregnation and pyrolysis (PIP), in order to provide the high dense matrix of SiC phases [4–6]. The LPS process is recognized as an attractive method for the high density of monolithic SiC and SiC_f/SiC composite materials, since the additive material can be transformed into some eutectics between SiC particles at the consolidation temperature lower than that of solid state sintering. The previous work showed that the mechanical properties of LPS-SiC materials greatly depended on the composition condition of Al_2O_3–Y_2O_3 additive materials [7]. The utilization of nanosize SiC powder was also effective for improving the mechanical properties of LPS-SiC_f/SiC composites [8,9]. However, the production condition of SiC matrix such as additive type, blending route and sintering temperature must be further optimized for improving the performance of LPS-SiC_f/SiC composites. Especially, in order to extend the fusion application of LPS-SiC based materials, the relationship between mechanical property and microstructure by the addition of fine oxide materials must be investigated at the elevated temperatures.

The purpose of the present study is to investigate the effect of test temperatures on the mechanical properties of monolithic LPS-SiC and LPS-SiC_f/SiC composite materials, in conjunction with the analysis of their microstructures. The fracture surface is also observed to explain the strength variation of LPS-SiC based materials.

2. Experimental procedures

The average sizes of commercial SiC powder for the fabrication of monolithic LPS-SiC and LPS-SiC_f/SiC composite materials were about 30 nm and about 0.3 μm, respectively. The sintering additives for LPS-SiC based materials were commercial Al_2O_3 and Y_2O_3 particles, which create secondary phases around starting SiC particles. The average sizes of Al_2O_3 and Y_2O_3 particles were about 1 and about 2 μm, respectively. The complex mixture containing SiC, Al_2O_3, Y_2O_3 and acetone was prepared by the blending speed of 160 rpm for 12 h, using a ball milling device. The total amount ($Al_2O_3 + Y_2O_3$) and the compositional ratio (Al_2O_3/Y_2O_3)

* Corresponding author. Tel.: +82 51 890 1662; fax: +82 51 890 2232.
E-mail address: splee87@deu.ac.kr (S.P. Lee).

0022-3115/$ - see front matter © 2008 Elsevier B.V. All rights reserved.
doi:10.1016/j.jnucmat.2008.12.164

of additive materials in the complex mixture were 10 wt% and 1.5, respectively. Such a blending condition of additive materials was determined for the proper dispersion of secondary phases, based on the results of previous work [7,10]. The plain woven fabrics of uncoated Tyranno SA SiC fiber (Ube Ltd., Japan) were used for the fabrication of LPS-SiC_f/SiC composites. A porous compact preform for LPS-SiC_f/SiC composites was prepared by the impregnation of complex mixture slurry into fabric structures of ten layers mounted in a rectangular shaped mold, using a gas pressure of 6.0 MPa. A rectangular compact body for LPS-SiC materials was also prepared by the same infiltration procedure of complex mixture slurry. LPS-SiC based materials were fabricated at the temperatures of 1820 °C under an applied pressure of 20 MPa for 2 h. The sintering temperature for the creation of liquid phases was determined from the phase diagram of Al_2O_3–Y_2O_3 system.

The microstructure for LPS-SiC and LPS-SiC_f/SiC composite materials was observed by a scanning electron microscope (SEM), after a mechanical polishing by diamond powders. Especially, the X-ray diffraction (XRD) analysis was carried out to identify the secondary phases of additive materials in the morphology of LPS-SiC materials. The sintering densities of LPS-SiC based materials were determined by the Archimedes' method. In order to examine the high temperature properties of LPS-SiC based materials, the four point bending test was performed at the temperatures of 1000 and 1200 °C under an argon atmosphere containing the oxygen partial pressure of 0.01 Pa. The bending load for composite materials was applied to upper portion of stacking layer structure. The test sample was maintained at each test temperature for 1 h after the heating of about 4 h. The dimensions of test samples for LPS-SiC and LPS-SiC_f/SiC composite materials was $2(t) \times 6 \times 40\ mm^3$. The span length and the crosshead speed for the bending tests of all materials were 32 mm and 0.5 mm/min, respectively.

3. Results and discussion

3.1. Microstructure and sintered density

Fig. 1 shows the representative microstructures of LPS-SiC materials. The microstructure of LPS-SiC materials exposed at the bending test temperature of 1200 °C was also shown in this figure. The thermal exposure time for LPS-SiC materials was 5 h. LPS-SiC materials without the thermal exposure represented a dense morphology, even if there were some amount of micropores. The morphology of LPS-SiC materials was mainly composed of SiC phase and secondary phase (white portion) by the chemical reaction of Al_2O_3 and Y_2O_3 particles. Large areas of secondary phases are also dispersed around SiC particles. However, the microstructure of LPS-SiC materials was affected by the thermal exposure history, corresponding to the duration of the bend test. In other words, the micropores in the microstructure of LPS-SiC materials increased due to the thermal exposure.

Fig. 2 shows the XRD results for LPS-SiC materials depending on the thermal exposure of bending test. LPS-SiC materials was heated for about 5 h at the temperature of 1200 °C. LPS-SiC materials without the thermal exposure mainly represented the peaks of SiC and secondary phases like $Y_3Al_2(AlO_4)_3$ in the microstructure. However, some amount of $AlYO_3$ phases were created in the microstructure of LPS-SiC materials, after the thermal exposure at the test temperature of 1200 °C. This is maybe because the increase of test temperature activates the chemical reaction of Al_2O_3 and Y_2O_3 particles, accompanying the formation of gas species such as CO, SiO and Al_2O [11].

Fig. 3 shows the optical microstructure of LPS-SiC_f/SiC composites reinforced with plain woven Tyranno SA fibrics. LPS-SiC_f/SiC composites showed a dense morphology with some pores, even if

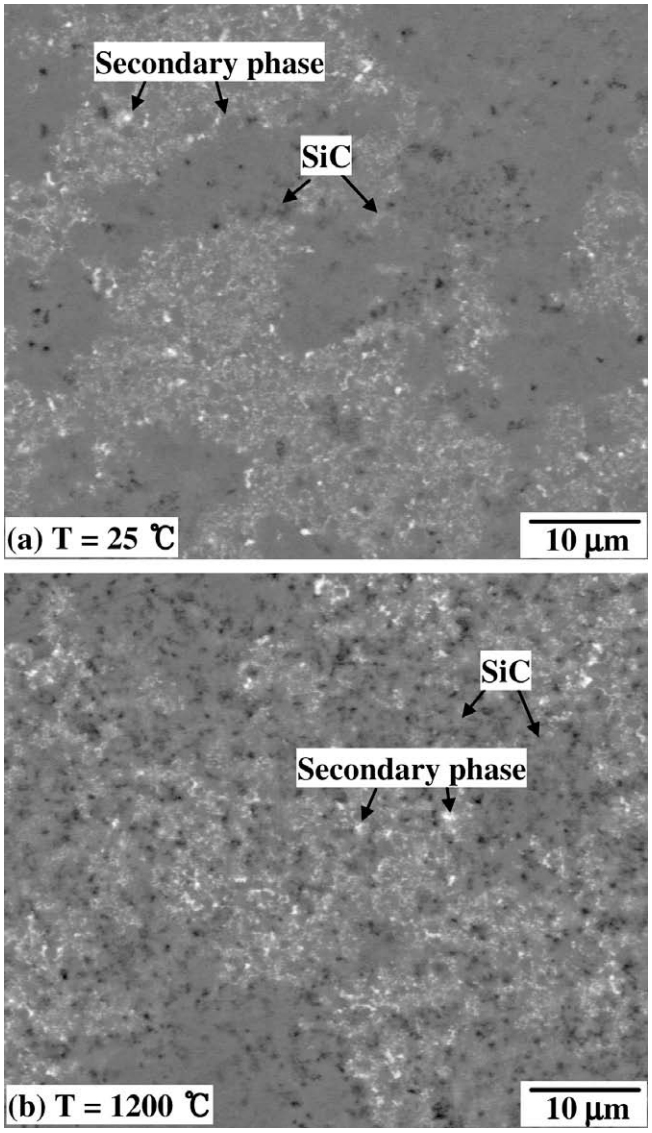

Fig. 1. Microstructures of LPS-SiC materials depending on the thermal exposure of bending test.

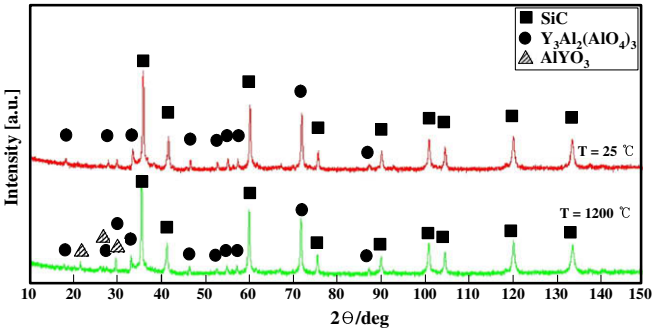

Fig. 2. XRD results for LPS-SiC materials depending on the thermal exposure of bending test.

there were some amount of delamination between the intersection of fiber bundles. However, the matrix slurry impregnated into intra-fiber bundles was transformed to dense SiC matrix (see Fig. 4(b)). As shown in Fig. 4(c), the detectable cracking of fiber

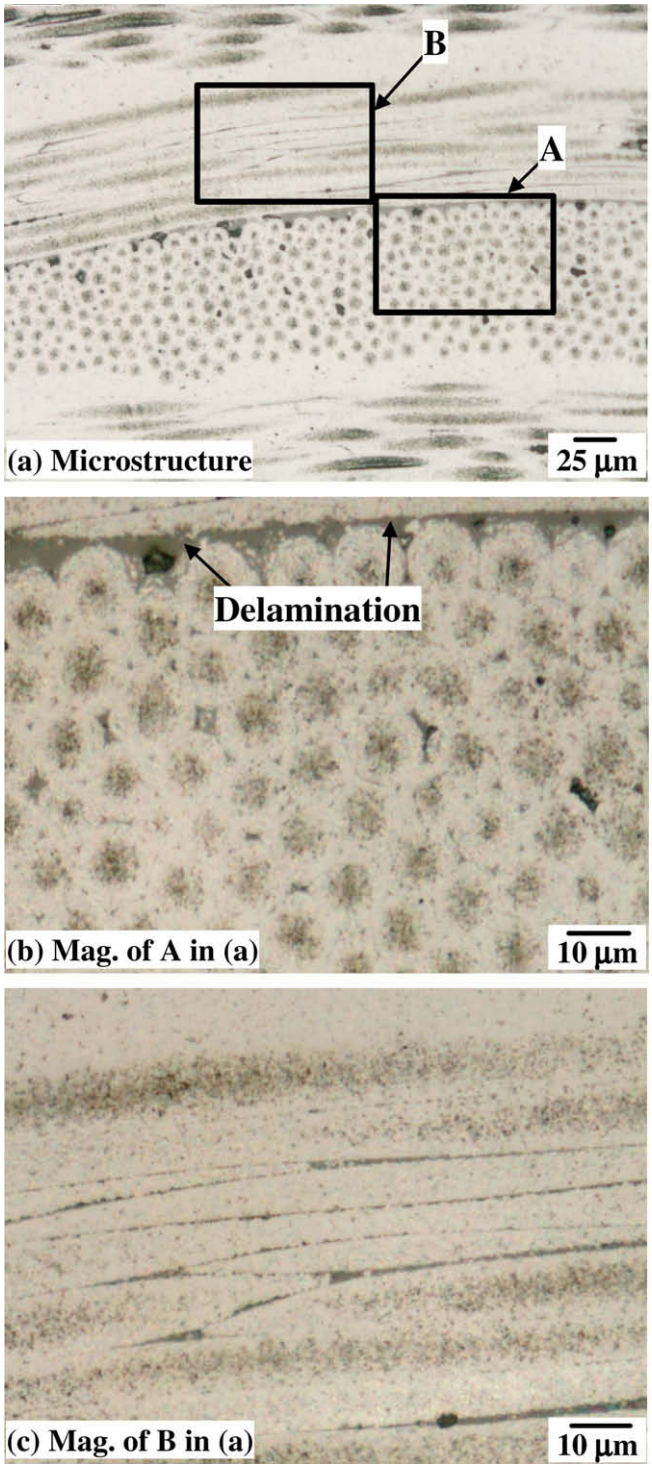

Fig. 3. Optical microstructures of LPS-SiC$_f$/SiC composites.

by the infiltration of matrix slurry and the hot-pressing process was not observed in the cross section of fibers. LPS-SiC$_f$/SiC composites represented an average density of about 3.1 Mg/m^3, which was higher than that of reaction sintered SiC$_f$/SiC composites by the infiltration of molten silicon [4].

Fig. 4 shows the effect of thermal exposure temperature on the sintered density and the porosity volume fraction of LPS-SiC materials. LPS-SiC materials was maintained for about 5 h at the bending test temperature. It was found that the LPS process by the addition of Al_2O_3–Y_2O_3 particles could provide an excellent density

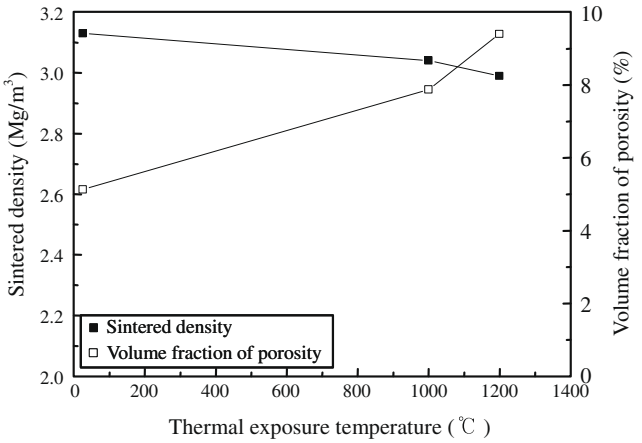

Fig. 4. Effect of thermal exposure temperature on the sintered density and the porosity volume fraction of LPS-SiC materials.

for monolithic SiC materials. LPS-SiC materials represented a density of about 3.1 Mg/m^3 and a porosity volume fraction of about 5% at the temperature of 25 °C. Such a density level corresponded to about 95% of theoretical density. Especially, the density of LPS-SiC materials was affected by the thermal exposure temperature. In other words, the density of LPS-SiC materials tended to decrease with the increase of thermal exposure temperature, accompanying to the increase of porosity volume fraction in the microstructure. LPS-SiC materials had a porosity volume fraction of about 10%, after the thermal exposure at the test temperature of 1200 °C. Such an increase of porosity volume fraction by the thermal exposure is related with the variation of secondary phases (see Fig. 2) and the active oxidation of SiC phase by the oxygen partial pressure (0.01 Pa) in the test atmosphere [7,11].

3.2. Mechanical properties

Fig. 5 shows the effect of bending test temperature on the flexural strength of LPS-SiC materials. LPS-SiC materials exhibited a typical brittle fracture behavior. LPS-SiC materials had an average flexural strength of about 750 MPa at the bending test temperature of 25 °C. Such a strength of LPS-SiC materials greatly decreased with the increase of test temperature. Especially, LPS-SiC materials represented a flexural strength of about 200 MPa at the bending

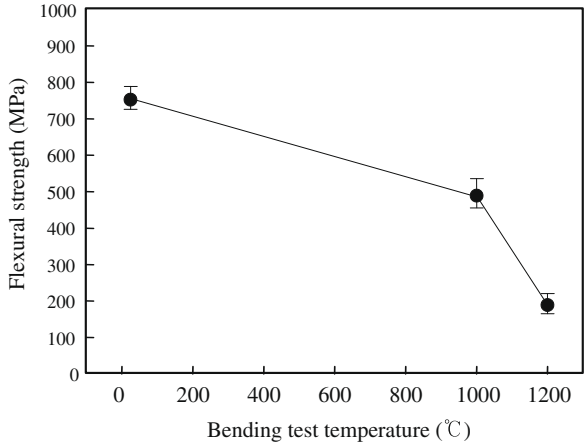

Fig. 5. Effect of thermal exposure temperature on the flexural strength of LPS-SiC materials.

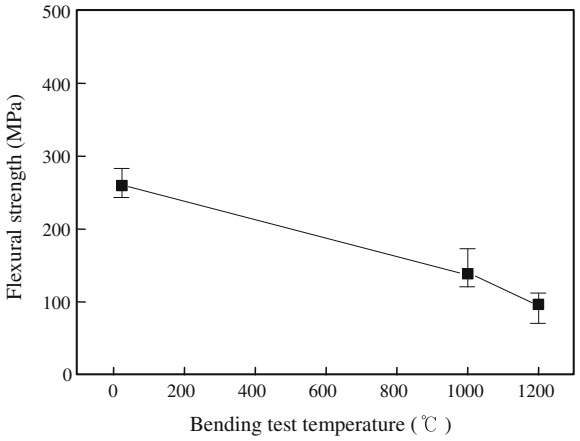

Fig. 6. Effect of bending test temperature on the flexural strength of LPS-SiC_f/SiC composites.

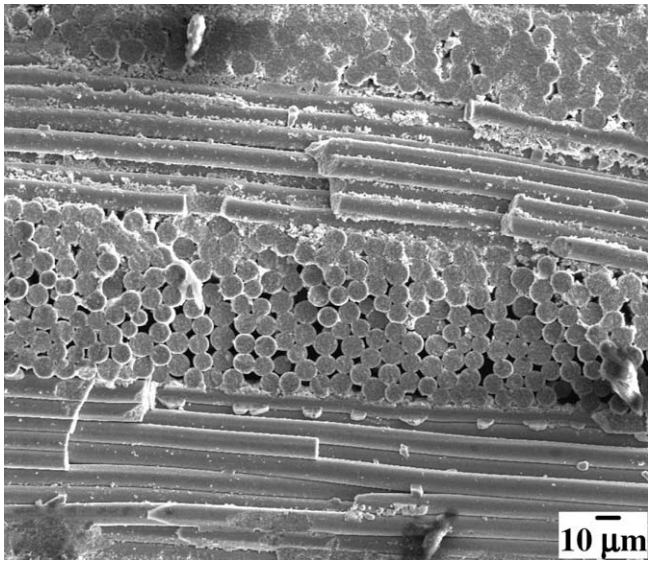

Fig. 7. Fracture surface of LPS-SiC_f/SiC composites tested at the temperature of 1200 °C.

test temperature of 1200 °C, which corresponded to about 25% of that at the test temperature of 25 °C. This is related with the damage of microstructure by the thermal exposure at the bending test temperature. That is to say, as shown in Figs. 1 and 4, the strength reduction of LPS-SiC materials was due to the increase of porosity in the microstructure. The reduction of loading capacity at the grain boundary by the enhancement of residual stress can be also considered as another factor for the degradation of LPS-SiC materials, since the secondary phase has a CTE higher than that of SiC [12].

Fig. 6 shows the effect of bending test temperature on the flexural strength of LPS-SiC_f/SiC composites. LPS-SiC_f/SiC composites showed a brittle fracture behavior due to the absence of interfacial coating layer, regardless of the bending test temperature. LPS-SiC_f/SiC composites represented a poor flexural strength of about 270 MPa at the bending test temperature of 25 °C, owing to the sintering defect between the intersection of fiber bundles (see Fig. 4). The increase of bending test temperature also led to the linear reduction of flexural strength in LPS-SiC_f/SiC composites. This is due to the degradation of SiC phase and fiber bundle region. LPS-SiC_f/SiC composites possessed a porosity volume fraction of about 15% at the bending test temperature of 1200 °C, which corresponded to three times of that at the bending test temperature of 25 °C. As shown in Fig. 7, LPS-SiC_f/SiC composites also exhibited a clear debonding of fiber bundles without fiber pull-outs at the bending test temperature of 1200 °C. It could be considered that such a microstructural damage decreased the high temperature strength of LPS-SiC_f/SiC composites.

4. Conclusions

LPS-SiC materials represented a good morphology with the density of about 3.1 Mg/m^3, even if there were some amounts of micropores. The density of LPS-SiC materials tended to decrease with the increase of thermal exposure temperature suffered from the bending test. The secondary phase like $Y_3Al_2(AlO_4)_3$ also created around SiC phases, due to the chemical reaction of Al_2O_3 and Y_2O_3 particles. The flexural strength of LPS-SiC materials greatly decreased with the increase of bending test temperature, owing to the creation of large amount of porosity. However, LPS-SiC materials represented a good flexural strength of about 750 MPa at the bending test temperature of 25 °C, which corresponded to four times of that at the bending test temperature of 1200 °C.

LPS-SiC_f/SiC composites exhibited a dense morphology of SiC matrix in the intra-fiber bundle region, when the fiber perform was prepared by the impregnation of matrix slurry into the fabric structure. LPS-SiC_f/SiC composites represented an average density of about 3.1 Mg/m^3 and an average flexural strength of about 270 MPa at the bending test temperature of 25 °C. Such a flexural strength of LPS-SiC_f/SiC composites linearly decreased with the increase of bending test temperature. This is caused by the microstructural damages associated with the degradation of SiC matrix by the increase of porosity and the debonding at the intersection of fiber bundles.

References

[1] A. Kohyama, M. Seki, A. Abe, T. Muroga, H. Matsui, S. Jistukawa, S. Matsuda, J. Nucl. Mater. 283–287 (2000) 20.
[2] B. Riccardi, L. Giancarli, A. Hasegawa, Y. Katoh, A. Kohyama, R.H. Jones, L.L. Snead, J. Nucl. Mater. 329–333 (2004) 56.
[3] J.S. Park, A. Kohyama, T. Hinoki, K. Shimoda, Y.H. Park, J. Nucl. Mater. 367–370 (2007) 719.
[4] S.P. Lee, J.O. Jin, J.S. Park, A. Kohyama, Y. Katoh, H.K. Yoon, D.S. Bae, I.S. Kim, J. Nucl. Mater. 329–333 (2004) 534.
[5] S. Dong, Y. Katoh, A. Kohyama, J. Eur. Ceram. Soc. 23 (2003) 1223.
[6] M. Kotani, A. Kohyama, Y. Katoh, J. Nucl. Mater. 289 (2001) 37.
[7] S.P. Lee, Y.S. Shin, D.S. Bae, B.H. Min, J.S. Park, A. Kohyama, Fus. Eng. Des. 81 (2006) 963.
[8] Y. Katoh, S.M. Dong, A. Kohyama, Fus. Eng. Des. 61 (2002) 723.
[9] J.S. Park, Y. Katoh, A. Kohyama, J.K. Lee, J.J. Sha, H.K. Yoon, J. Nucl. Mater. 329–333 (2004) 558.
[10] S.P. Lee, Y.S. Shin, J.K. Lee, J.H. Lee, J.Y. Park, Key Eng. Mater. 326–328 (2006) 1853.
[11] S. Baud, F. Thevenot, A. Pisch, C. Chatillon, J. Eur. Ceram. Soc. 23 (2003) 1.
[12] J.H. She, K. Ueno, Mater. Chem. Phys. 59 (1999) 139.